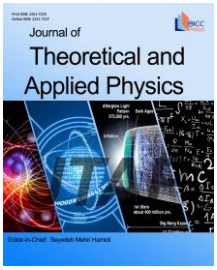

J. Theor. Appl. Phys., 2026; 20(4): 403-413

Journal of Theoretical and Applied Physics (JTAP)

https://doi.org/10.57647/jtap.2026.2004.06

Research Article

# First-Principles Investigation of the Structural, Electronic, and Optical Properties of $Tl_{1-x}B_xN$ Alloys in the Zinc-Blende Phase

Abed Zoulikha*, Abdelali Laid*, Lachabi Abdelhadi, Abid Hamza

*Applied Materials Laboratory, Research Center, Sidi Bel Abbes University, 22000, Algeria*

***Corresponding author:** zoulikhaabed3@gmail.com, laid.abdelali@univ-sba.dz

**Article History:**

Received:
04 February 2026

Revised:
25 February 2026

Accepted:
04 April 2026

Published online:
17 April 2026

Published in Issue:
31 August 2026



**Abstract**

In this work, a comprehensive first-principles investigation of the structural, electronic, and optical properties of $Tl_{1-x}B_xN$ (x = 0.25, 0.50, and 0.75) alloys crystallizing in the zinc-blende phase is presented. To the best of our knowledge, a systematic theoretical study of these ternary alloys combining structural optimization, electronic structure analysis, and optical response including spin–orbit coupling effects has not been reported previously. The calculations were performed within density functional theory using the generalized gradient approximation. The optimized lattice parameters were obtained from total energy–volume calculations and exhibit a composition-dependent trend consistent with Vegard's law, confirming the structural stability of the considered alloys. The electronic band structures reveal a pronounced dependence of the band gap on boron concentration, demonstrating the possibility of band gap engineering through composition tuning. The inclusion of spin–orbit coupling leads to a noticeable modification of the electronic structure and a reduction in the band gap, reflecting the significant relativistic effects associated with thallium atoms. The optical properties were analyzed in the photon energy range of 0 - 14 eV. The calculated dielectric function, absorption coefficient, refractive index, and reflectivity show strong sensitivity to boron content, indicating tunable optical behavior. Overall, the results highlight the potential of $Tl_{1-x}B_xN$ alloys for advanced optoelectronic and photonic applications, particularly in tunable semiconductor and ultraviolet device technologies.

**Keywords:** $Tl_{1-x}B_xN$ alloys, Zinc-blende phase, Band gap engineering, Spin–orbit coupling, Optical properties, Dielectric function, Optoelectronic materials

**Cite this article:** Abed, Z., Abdelali, L., Lachabi, A. & Abid, H., (2026). First-Principles Investigation of the Structural, Electronic, and Optical Properties of $Tl_{1-x}B_xN$ Alloys in the Zinc-Blende Phase. *J. Theor. Appl. Phys.,* 20(4), 403-413. https://doi.org/10.57647/jtap.2026.2004.06

## 1. Introduction

Compound semiconductors are among the fundamental building blocks for modern optical and electronic technologies due to their high tunability of structural, electronic, and optical properties through adjustments in chemical composition and crystal structure. In this context, $Tl_{1-x}B_xN$ alloys are of particular interest, given the scarcity

of both theoretical and experimental studies on these materials.

Incorporating thallium, with its distinctive electronic characteristics, into boron-based nitrides offers a promising route to engineer the band gap, refractive index, and spectral absorption properties, while also influencing structural parameters and electronic behavior. These features make $Tl_{1-x}B_xN$ alloys strong candidates for applications in solar cells, photodetectors, and optical communication devices.

Previous studies on similar systems have shown that varying the chemical composition can significantly alter their optical, electronic, and structural characteristics.

For instance, in $Ga_{1-x}In_xSb$ alloys, increasing indium concentration leads to a higher static dielectric constant, consistent with a reduction in band gap energy, while the onset and main peaks in the imaginary part of the dielectric function closely follow the corresponding band gap values [1].

Likewise, investigations on $BN_xAs_{1-x}$ alloys have demonstrated that the refractive index and optical dielectric constant vary nonlinearly with nitrogen content, reflecting the complex influence of composition on optical response [2]. Furthermore, studies on TlInN have shown that incorporating thallium results in a linear decrease in the band gap with increasing Tl content, accompanied by noticeable changes in lattice parameters, suggesting that Tl-containing InN systems are promising for optical and optoelectronic applications in the infrared range [5]. In $TlxGa_{1-x}As$ alloys with $x < 0.75$, the direct band gap semiconductor nature is preserved, whereas compositions with $x \geq 0.75$ exhibit semi-metallic behavior. Significant changes in absorption, reflectivity, and refractive index were also reported, highlighting the considerable potential of these alloys for optoelectronic applications, particularly in infrared detection [3].

First-principles calculations comparing TlGaAs and InGaAs further demonstrated that $Tl_{0.25}Ga_{0.75}As$ exhibits higher quantum efficiency for infrared detection at a wavelength of approximately 2500 nm than its counterparts [4].

Additionally, $B_{1-x}Tl_xN$ alloys have been proposed as promising materials for both infrared and visible spectral ranges, as analysis of the dielectric function and refractive index revealed strong optical activity in these regions [6].

Moreover, the thallium content in compounds such as $TlxAl_{1-x}P$ has been shown to affect the curvature parameters of the electronic band gap, thereby influencing their optical properties [7].

Several theoretical studies have also investigated the electronic properties of zinc-blende semiconductor alloys using pseudopotential methods, demonstrating that the electronic parameters may vary non-linearly with alloy composition [28].

Based on this background, the present work aims to conduct a comprehensive study of the structural, electronic, and optical properties of $Tl_{1-x}B_xN$ alloys at different compositions, including the effects of spin–orbit coupling (SOC) on the electronic structure. Other important electronic parameters, such as electron and hole effective masses, which are crucial for carrier transport and device applications, will be addressed in a future study.

The findings are expected to contribute to the scientific understanding of these materials and open new possibilities for designing tailored optical and optoelectronic materials for future technological applications.

## 2. Computational method

The calculations were performed within the framework of density functional theory (DFT) by solving the Kohn–Sham equations using the full-potential linearized augmented plane wave (FP-LAPW) method as implemented in the WIEN2k simulation package [1, 8]. The exchange–correlation potential was described within the generalized gradient approximation (GGA) using the Perdew–Burke–Ernzerhof (PBE) parameterization [9]. In addition, the Engel–Vosko generalized gradient approximation (EV-GGA) was employed to provide a more accurate description of the electronic structure, particularly for the evaluation of electronic and optical properties [26].

The compounds were modeled in the zinc-blende (ZB) structure.

To simulate different boron concentrations ($x = 0.25$, 0.5, and 0.75), a 2×2×2 supercell was constructed. Selected boron (B) atoms were replaced by thallium (Tl) atoms to achieve the desired compositions while preserving periodic boundary conditions and crystal symmetry [10].

The muffin-tin radii (RMT) were carefully chosen to avoid sphere overlap, and the plane-wave cutoff parameter was set to $R_{MT} \cdot K_{max} = 7.0$.

The energy cutoff separating core and valence states was fixed at –6.0 Ry.

Brillouin zone integrations were performed using a Monkhorst–Pack k-point mesh of 11×11×11, corresponding to 56 irreducible k-points [11].

The valence electronic configurations of the constituent atoms were considered as follows: Tl: [Xe] $4f^{14}5d^{10}6s^26p^1$, B: [He] $2s^22p^1$, and N: [He] $2s^22p^3$.

These configurations ensure the inclusion of orbitals that mainly contribute to interband transitions, particularly the Tl 6p states, which play a significant role in the formation of the conduction band [12].

Finally, the optical properties of all investigated compounds were calculated in the photon energy range of 0–14 eV.

## 3. Results and discussion

### 3.1. Structural properties

The optimized lattice parameter (a) and bulk modulus ($B_0$) of $Tl_{1-x}B_xN$ alloys calculated within the GGA and GGA+SOC approximations are summarized in Table 1. The structural parameters were obtained through a geometry optimization procedure in which the total energy of the unit cell was minimized with respect to the unit cell volume within the GGA-PBE approximation [27]. From the obtained results, it is clearly observed that the lattice constant decreases progressively with increasing boron concentration (x = 0.25–0.75).

Specifically, the lattice parameter decreases from 4.94675 Å for $Tl_{0.75}B_{0.25}N$ to 4.11640 Å for $Tl_{0.25}B_{0.75}N$ (GGA results).

This behavior can be attributed to the significant difference in atomic radii between Tl and B atoms, where boron has a much smaller atomic radius than thallium.

Consequently, increasing the boron content leads to a contraction of the crystal lattice.

In contrast, the bulk modulus ($B_0$) exhibits an opposite trend, increasing from 112.0870 GPa to 240.9058 GPa as the boron concentration increases.

This indicates that the material becomes mechanically harder and less compressible with higher boron content. The increase in $B_0$ suggests stronger bonding interactions due to the shorter bond lengths and the enhanced covalent character introduced by boron atoms.

The inclusion of spin–orbit coupling (SOC) produces only minor variations in the lattice parameter and bulk modulus, indicating that SOC has a negligible influence on the structural properties of $Tl_{1-x}B_xN$ alloys.

This behavior is expected since SOC mainly affects the electronic structure rather than the equilibrium geometry. The total energy values confirm the stability of the optimized structures for all studied compositions. To the best of our knowledge, no previous theoretical or experimental studies have reported structural data for $Tl_{1-x}B_xN$ alloys in the zinc-blende phase. Therefore, a direct comparison with earlier results is not possible, and the present calculations may serve as reference data for future investigations.

As shown in Table 1, the inclusion of spin–orbit coupling (SOC) produces only minor variations in the lattice parameter and bulk modulus.

This confirms that SOC has a negligible effect on the structural properties of $Tl_{1-x}B_xN$ alloys.

The calculated total energy values further support the stability of the optimized structures for all studied compositions.

The gradual decrease in the lattice constant with increasing boron concentration can be primarily attributed to the large difference in atomic radii between boron and thallium. Since the boron atom is considerably smaller than thallium, its incorporation into the lattice leads to a contraction of the crystal structure [25].

This behavior is approximately consistent with Vegard's law [24], indicating a nearly linear variation of the lattice parameter with composition.

Furthermore, the reduction in crystal volume is accompanied by a strengthening of the interatomic interactions due to the enhanced overlap of electronic orbitals.

This increase in the electronic density within the bonds results in a higher bulk modulus ($B_0$). Therefore, as the boron concentration increases in $Tl_{1-x}B_xN$ alloys, the material becomes mechanically stiffer and less compressible, reflecting an improvement in structural cohesion.

The compositional dependence of the lattice parameter and bulk modulus is further illustrated in Figures 1 and 2. The nearly linear variation of the lattice constant confirms the approximate validity of Vegard's law, while the monotonic increase in the bulk modulus ($B_0$) reflects the progressive strengthening of interatomic bonding with increasing boron concentration.

**Table 1.** Optimized structural parameters of $Tl_{1-x}B_xN$ alloys in the zinc-blende phase calculated using GGA and GGA+SOC methods

| Material | Method | a (A°) | $B_0$ (GPa) | E (Ry) |
|---|---|---|---|---|
| $Tl_{075}B_{0.25}N$ | GGA | 4.94675 | 112.0870 | -244441.590256 |
| | GGA+ SOC | 4.94805 | 110.3503 | -244438.112667 |
| $Tl_{0.5}B_{0.5}N$ | GGA | 4.45280 | 178.2332 | -163382.687595 |
| | GGA+ SOC | 4.45525 | 182.1452 | -163383.243294 |
| $Tl_{0.25}B_{0.75}N$ | GGA | 4.11640 | 240.9058 | -82328.301905 |
| | GGA+ SOC | 4.1176 | 246.2844 | -82328.522996 |

10.57647/jtap.2026.2004.06

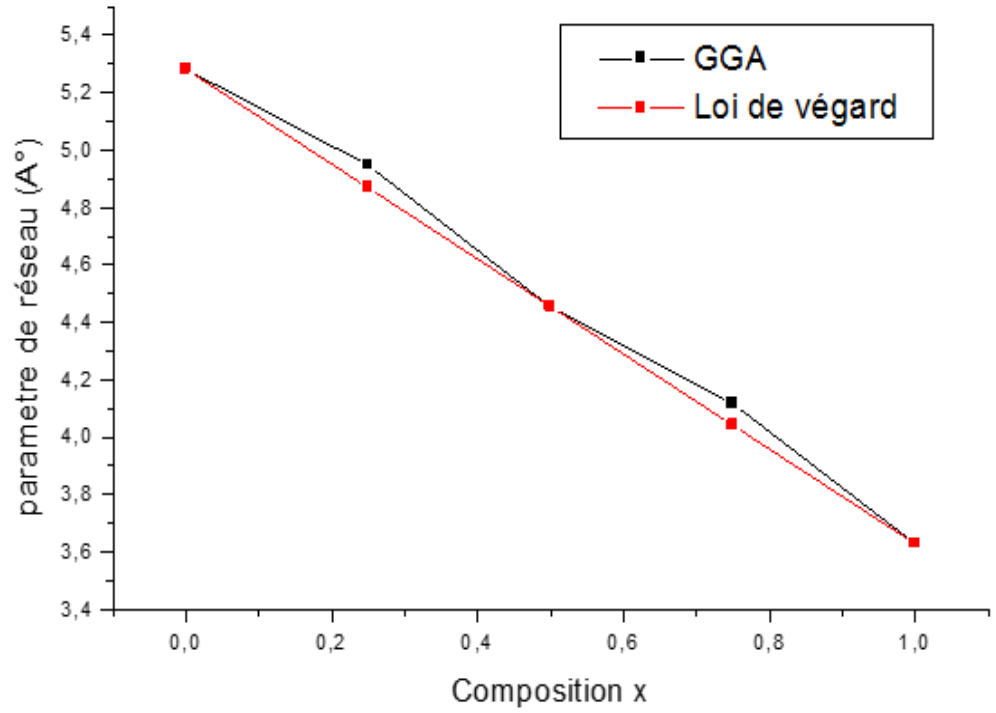


**Figure 1.** Calculated lattice constant of the $Tl_{1-x}B_xN$ alloy as a function of composition, compared with Vegard's law

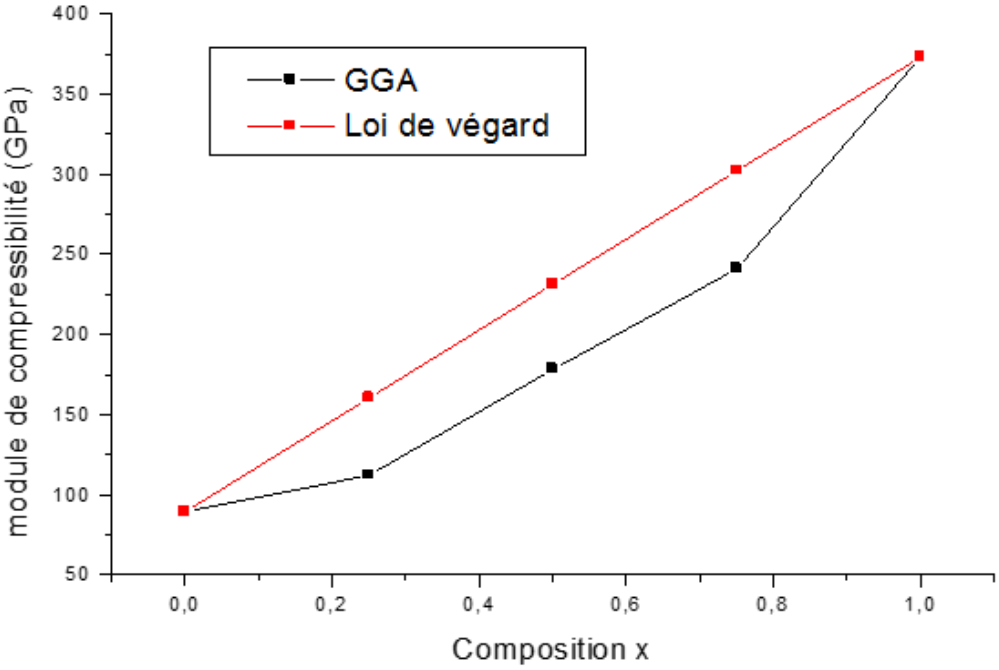


**Figure 2.** Calculated bulk modulus of the $Tl_{1-x}B_xN$ alloy as a function of composition

### 3.2. Electronic properties

The study of the electronic properties of $Tl_{1-x}B_xN$ alloys is essential for understanding the behavior of these ternary compounds, which combine elements with strong contrasts in electronegativity and atomic size, namely thallium and boron. In the zinc-blende structure, the energy band distribution results from a significant hybridization between the heavy thallium orbitals and the lighter boron contributions, making the band gap particularly sensitive to the computational approach employed. Therefore, the analysis of the band structure and the electronic density of states (DOS) was carried out using the GGA approximation, both with and without spin–orbit coupling (SOC). This comparative approach allows us to highlight the influence of SOC on the band edges and provides a clear baseline for understanding the electronic behavior of $Tl_{1-x}B_xN$ alloys as a function of boron concentration.

10.57647/jtap.2026.2004.06

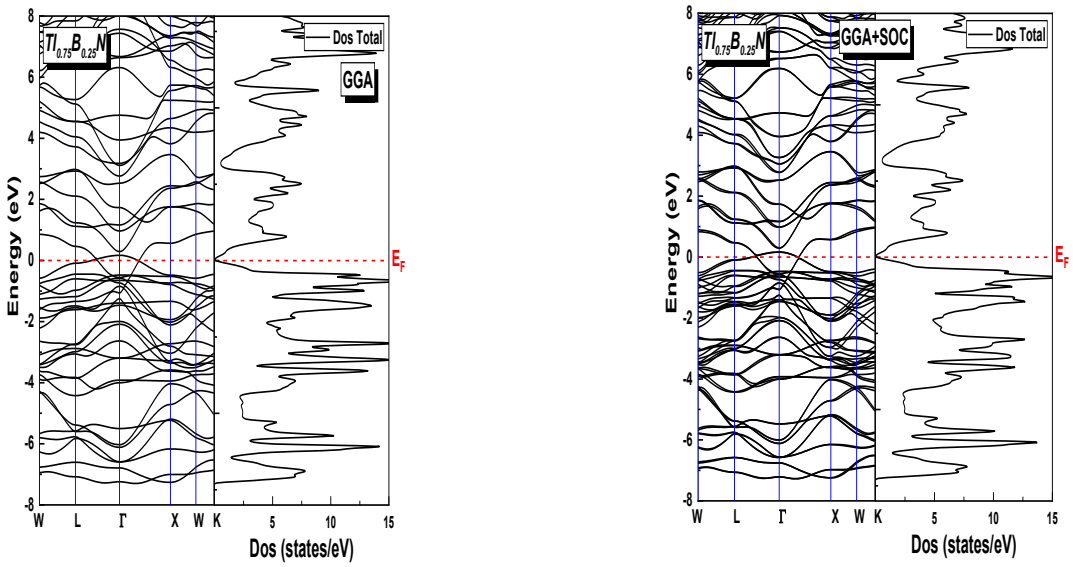


(a)

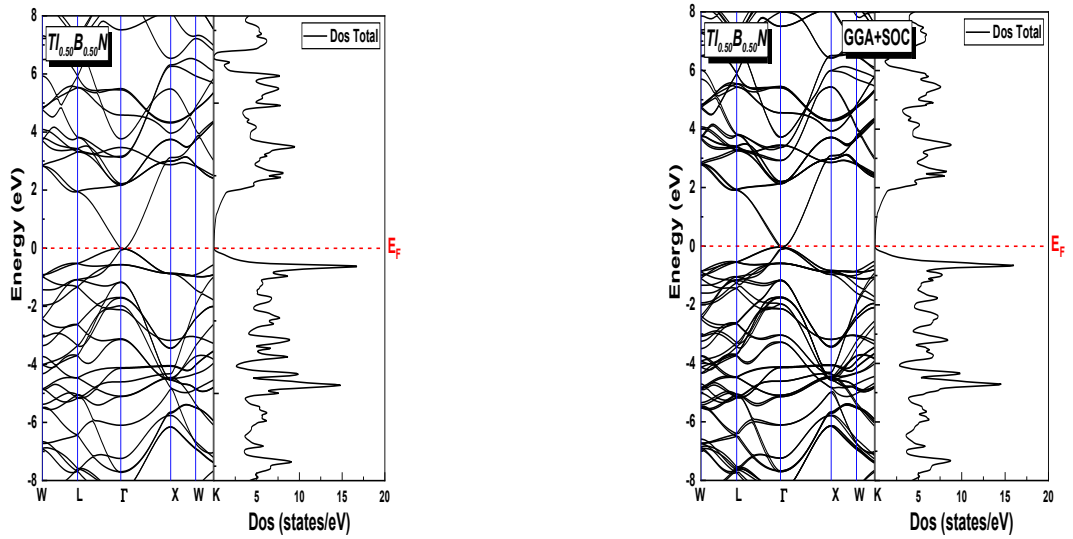


(b)

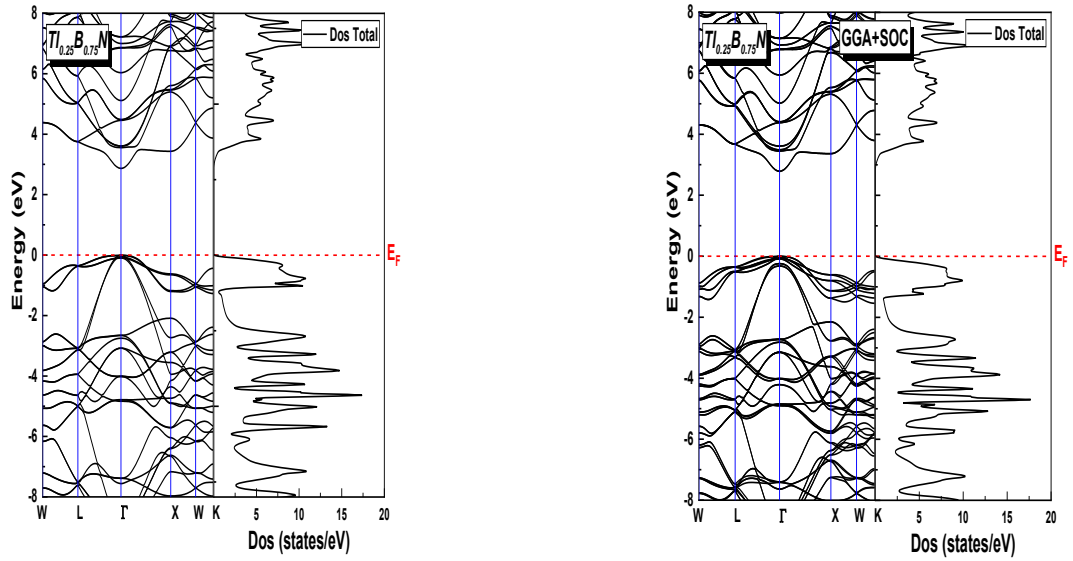


(c)

**Figure 3.** Band structures and total density of states (DOS) of $Tl_{1-x}B_xN$ alloys for different boron concentrations (x = 0.25, 0.5, 0.75) calculated using GGA and GGA+SOC: (a) x = 0.25, (b) x = 0.5, (c) x = 0.75

10.57647/jtap.2026.2004.06

**Table 2.** Calculated band gaps ($E_g$) at the Γ–Γ point for $Tl_{1-x}B_xN$ alloys using GGA and GGA+SOC

| Material | $Eg^{\Gamma-\Gamma}$ (eV) | |
|---|---|---|
| | GGA | GGA+SOC |
| $Tl_{0.75}B_{0.25}N$ | Semi-metal | Metal |
| $Tl_{0.5}B_{0.5}N$ | Semi-metal | Semi-metal |
| $Tl_{0.25}B_{0.75}N$ | 2.86557 | 2.78433 |

The calculated band structures, along with the total density of states (DOS), for all studied boron concentrations are illustrated in Figure 3.

Figure 3 presents the results for (a) x = 0.25, (b) x = 0.5, and (c) x = 0.75. Although DOS is included in the figure, the focus here is on the evolution of the conduction and valence bands, which clearly demonstrates the transition from semi-metallic to semiconducting behavior with increasing boron content

The calculated band gaps at the Γ–Γ point are summarized in Table 2. For the lowest boron concentration (x = 0.25), the alloy exhibits semi-metallic behavior under both GGA and GGA+SOC approximations, indicating a negligible or zero band gap. This is attributed to the dominance of thallium orbitals in the conduction band, which strongly hybridize with the valence states, leading to band overlap and metallic character. At an intermediate composition (x = 0.5), the alloy remains semi-metallic, suggesting that the increasing boron content is not yet sufficient to open a significant band gap. The electronic structure in this regime reflects a competition between the small atomic radius and high electronegativity of boron, which tends to localize the valence states, and the delocalized thallium orbitals, which favor metallic conduction. For the highest boron concentration (x = 0.75), a direct band gap emerges at the Γ point, with values of 2.86557 eV for GGA and 2.78433 eV for GGA+SOC.

The slight reduction in the band gap when including SOC indicates that relativistic effects slightly perturb the conduction band minimum and valence band maximum, without drastically changing the overall electronic nature of the alloy. The opening of the band gap with increasing boron content can be attributed to the smaller atomic size and higher electronegativity of boron compared to thallium, which enhances orbital localization and increases the energy separation between valence and conduction bands.

Overall, these results reveal a composition-dependent transition from semi-metallic to semiconducting behavior in $Tl_{1-x}B_xN$ alloys. This trend suggests that tuning the boron concentration is an effective strategy to engineer the band gap, which is critical for potential applications in optoelectronic devices, such as infrared detectors and solar cells. Moreover, the minor effect of SOC implies that relativistic corrections primarily influence the fine structure of electronic states, rather than the overall band gap magnitude.

### 3.3. Optical properties

Before analyzing the optical properties of the $Tl_{1-x}B_xN$ alloys, it is relevant to briefly recal the key electronic features obtained from our structural optimization, performed within the GGA approximation, and subsequent band structure calculations. For the composition with x=0.75, the results reveal a direct semiconducting gap of Eg≈2.87 eV (Γ-Γ transition), whereas the alloys with x=0.25 and x=0.50 display a semi metallic character with negligible band separation. These differences in the electronic nature are expected to govern the onset of interband transitions and, therefore, have a strong influence on the optical response. A detailed investigation of the structural and electronic properties will be presented in a separate scientific article, while the present work focuses exclusively on the optical behavior. Based on these electronic trends; the following sections present and discuss the calculated dielectric function, refractive indices, absorption coefficients, reflectivity, and energy-loss spectra for the studied compositions.

To accurately interpret these optical properties, we first present the fundamental equations used to calculate the key optical parameters, starting with the dielectric function:

$$\varepsilon(\omega) = \varepsilon_1(\omega) + i\varepsilon_2(\omega) \quad (1)$$

The imaginary part $\varepsilon_2(\omega)$ was computed using the momentum matrix elements between occupied and unoccupied states, while the real part $\varepsilon_1(\omega)$ was obtained by applying the *Kramers-kronig* transformation [13]. all calculations were performed with high precision, using a total energy convergence criterion of $10^{-4}$Ry. As previously mentioned, this work provides a detailed presentation and analysis of the main optical properties, such as the refractive index and the absorption coefficient, which are determined according to relations (2) and (3), respectively.

$$n(\omega) = \left[\frac{\varepsilon_1(\omega)}{2} + \frac{\sqrt{\varepsilon_1^2(\omega) + \varepsilon_2^2(\omega)}}{2}\right]^{1/2} \quad (2)$$

$$\alpha(\omega) = \frac{4\pi}{\lambda} k(\omega) \quad (3)$$

In these relations, k represents the extinction coefficient, while λ refers to the wavelength of light in vacuum. Further details on the methodology used to calculate these optical properties can be found in the works of *Ambrosch-Draxl* and Sofo [14, 15, 16]. On the other hand, the reflectivity R(ω) is one of the key optical parameters that reflects the interaction of light with the electronic structure of a

material. This parameter directly depends on both the real refractive index n(ω) and the absorption coefficient k(ω), and in the general case is given by:

$$R = \frac{(n-1)^2 + k^2}{(n+1)^2 + k^2} \quad (4)$$

In the special case whee the material is transparent or nearly transparent, i.e, when the absorption coefficient is neglected (k=0), the expression simplifies to:

$$R = \left(\frac{n-1}{n+1}\right) \quad (5)$$

Reflectance spectroscopy is a powerful technique for studying electronic systems, providing insights into interband transitions, band structure, and the material's intrinsic optical properties [17].

To check the optical properties of solids the energy –Loss function (L(ω)) is one of the most important quantities. The energy –Loss function is proportional to the probability of energy loss (E) in unit of length as an electron is moving through the environment and it is given by:

$$L(\omega) = lm\left(-\frac{1}{\varepsilon(\omega)}\right) = \frac{\varepsilon_2^2}{\varepsilon_1^2 + \varepsilon_2^2} \quad (6)$$

The primary peak in the energy-loss function, referred to as the Plasmon peak, reflects the excitation of the bulk charge density within the crystal.

In the design of optoelectronic devices, a precise understanding of key optical parameters is essential. These properties can be evaluated based on electronic transitions, as described by the time-dependent perturbation of the total electronic state [18].

Firstly, we will investigate the optical properties of $Tl_{1-x}B_xN$ Alloys at concentrations x= 0.25, 0.50, and 0.75, by analyzing the real $\varepsilon_1(\omega)$ and imaginary $\varepsilon_2(\omega)$ parts of the dielectric function, as well as the refractive index $n(\omega)$ over a wide energy range [0-14 eV].

This analysis will allow us to determine the effect of varying boron concentration on the optical response of the materials across different regions of the electromagnetic spectrum.

The calculated imaginary part $\varepsilon_2(\omega)$, the real part $\varepsilon_1(\omega)$ , and the refractive index are shown in Figure 4, 5 and 6 of $Tl_{0.75}B_{0.25}N$, $Tl_{0.5}B_{0.5}N$, and $Tl_{0.25}B_{0.75}N$ respectively.

The results revealed a gradual transition from semiconducting to semimetallic behavior with decreasing boron concentration.

For the compound at x= 0.75 ($Tl_{0.25}B_{0.75}N$), absorption starts at around 3 eV, with pronounced peaks in the range of 7-10.5 eV, indicating a direct band gap of about 3 eV. At x = 0.5 ($Tl_{0.5}B_{0.5}N$), absorption begins at lower energies (~1 eV) with a strong peak at 4 eV, then stabilizes at relatively low values within the 10-14 eV range, reflecting a semi metallic character.

In contrast, the compound at x = 0.25 ($Tl_{0.75}B_{0.25}N$) exhibits absorption nearly from zero with distinct peaks below 2.5 eV, followed by a gradual decrease up to 14 eV, confirming metallic behavior.

Moreover, the real part of the dielectric function at zero increases as the boron concentration decreases, taking values of 6, 9, and 19 for the three compounds, respectively.

The static imaginary dielectric constant in the studied compounds decreases as band gap increases [20].

In parallel, the Plasmon energy (where $\varepsilon_1$ vanishes) shifts from about 9.5 eV at x = 0.75 to ~7.1eV at x = 0.5, and further decreases to below 2.5 eV at x = 0.25. From our results, the compound with boron concentration x= 0.75 exhibits a clear energy band gap in the visible range and is consistent with Penn's model $\varepsilon_1(0) = 1 + (\frac{\hbar\omega p}{Eg})^2$ [22].

The static refractive index takes the values n (0) ≈ 2.5, 3.0, and 4.4 respectively, then gradually decreases with increasing photon energy, reaching its minimum around 14 eV, Overall, these results demonstrate that controlling the boron concentration enables tuning of the optical response of $Tl_{1-x}B_xN$ compounds, allowing the transition from a direct-gap semiconductor to a semimetal with strong plasmonic features.

This makes the series promising for advanced optical and photonic applications, in agreement with previous studies on ENZ phenomena and plasmons in similar systems [19].

After completing the study and analysis of the previously discussed optical properties, we proceed to examine and analyze the behavior of the remaining optical parameters, including the absorption coefficient, reflectivity, and energy loss function.

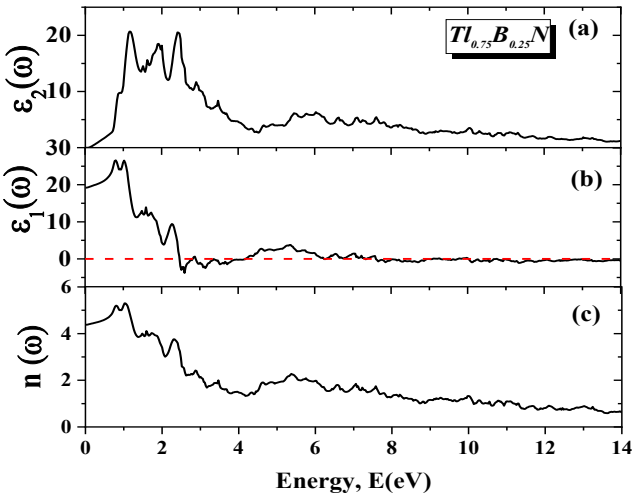


**Figure 4.** a, b, c. Real and Imaginary Parts of the Dielectric Function $\varepsilon_1(\omega)$ and $\varepsilon_2(\omega)$, and Refractive Index n(ω) of the $Tl_{0.75}B_{0.25}N$ compound

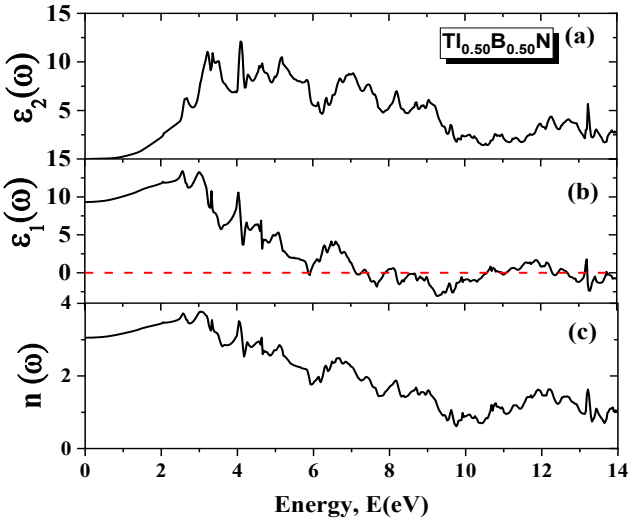


**Figure 5.** a, b, c. Real and Imaginary Parts of the Dielectric Function $\varepsilon_1(\omega)$ and $\varepsilon_2(\omega)$, and Refractive Index $n(\omega)$ of the $Tl_{0.5}B_{0.5}N$ compound

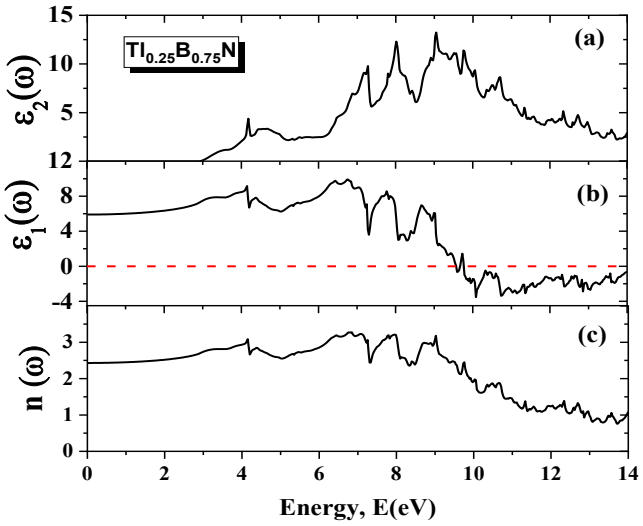


**Figure 6.** a, b, c. Real and Imaginary Parts of the Dielectric Function $\varepsilon_1(\omega)$ and $\varepsilon_2(\omega)$, and Refractive Index $n(\omega)$ of the $Tl_{0.25}B_{0.75}N$ compound

These quantities show evident variations in figures 7, 8, and 9, for the same compounds and for the concentrations 0.25, 0.5, and 0.75, respectively.

The absorption coefficient is one of the key properties of optoelectronic materials, defined as the amount of light absorbed per unit length of the material [18].

When optoelectronic materials absorb light, electrons are excited from one energy band to another.

A good absorber material can capture all incident electromagnetic radiation, allowing the complete excitation of electrons.

However, if the photon energy is lower than the material's bandgap, the light absorption to occur; the photon energy must be greater than the bandgap energy [20]. Through the study of the absorption coefficient of the $Tl_{1-x}B_xN$ compounds (x=0.75, 0.5, 0.25) it is evident that the optical behavior varies according to the boron concentration.

The $Tl_{0.75}B_{0.25}N$ compound exhibits the onset of absorption at a low photon energy of about 1 eV, reflecting early electronic transitions related to its semimetallic nature

Prominent peaks are also observed at higher energies (>10 eV) where the absorption exceeds $150\times10^4\ cm^{-1}$ which is associated with transitions between deep valence bands and the conduction band.

For $Tl_{0.5}B_{0..5}N$ compound absorption begins at a slightly higher energy (~1.3 eV) with strong peaks appearing in the 9.5-14eV range. the absorption intensity in this region surpasses $250x10^4cm^{-1}$ , indicating a high density of optical transitions in this energy domain .in contrast , the $Tl_{0.25}B_{075}N$ compound (semiconducting) requires a larger photon energy (~3eV) to initiate absorption , consistent with the nature of semiconductors possessing wider band gaps its most pronounced peaks occur at higher energies ( > 9eV) with values also exceeding $250x10^4\ cm^{-1}$ showing a trend similar to the other two compositions but shifted to higher energies. Regarding reflectivity the three compounds display clear differences at low photon energies (0eV), with values of about 0.4 for $Tl_{0.75}B_{0.25}N$, 0.25for $Tl_{0.5}B_{0.5}N$ and less than 0.2 for $Tl_{0.25}B_{0.75}N$. These results directly reflect the variation in electronic density at the Fermi level. Moreover, the reflectivity peaks correlate with those observed in the imaginary part of the dielectric function ($\varepsilon_2$) confirming the strong link between absorption and reflectivity.

It should be noted that plasma oscillation in metals or plasmas within the ultraviolet region always decouple from the lattice framework due to the rapid movements of electrons. This phenomenon explains why the plasmonic response appears independently of the crystal lattice and strongly influences both the absorption and reflectivity spectra [23]. For instance in $Tl_{0.75}B_{0.25}N$, a sharp drop occurs at 2.1 eV which coincides with the energy where $\varepsilon_1$ changes sign from positive, marking the onset of plasmonic response. For $Tl_{0.25}B_{0.75}N$ regular oscillations in reflectivity emerge starting from 3eV, which is the same energy at which absorption begins.

These oscillations persist at higher energies, with reflectivity reaching about 0.5 near 7 eV. As for the energy-loss spectra their evolution closely follows the trend of the absorption coefficient with the positions of the peaks coinciding with those in absorption this correspondence reflects the collective nature of electronic excitations (Plasmon excitations).The value of the electron energy-loss spectroscopy is related to the feature coupled with plasma oscillation [21].

From these findings it can be concluded that increasing boron content gradually drives the compounds from semi metallic toward semiconducting behavior which explains the differences observed in the onset of absorption and reflectivity among the three compositions.

10.57647/jtap.2026.2004.06

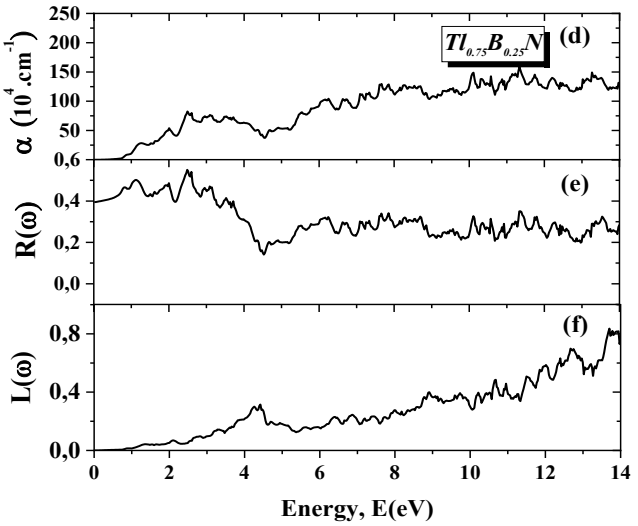


**Figure 7.** d, e, f. The absorption coefficient$\alpha(\omega)$, reflectivity R(ω), and energy loss function L(ω) of the $Tl_{0.75}B_{0.25}N$ compound

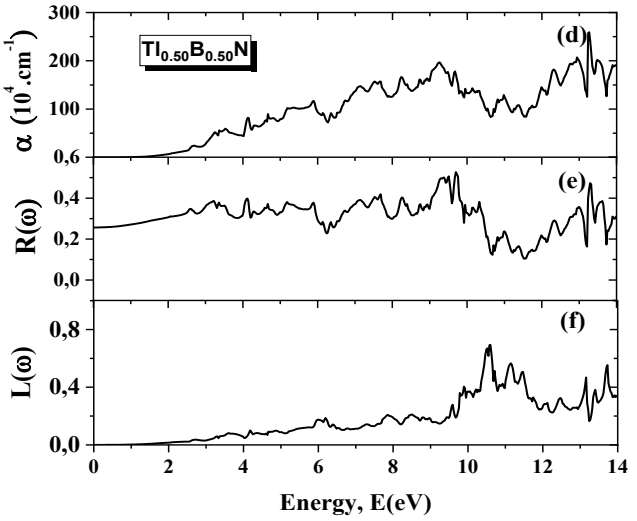


**Figure 8.** d, e, f. the absorption coefficient $\alpha(\omega)$, reflectivity R(ω), and energy loss function L(ω of the $Tl_{0.5}B_{0.5}N$ compound

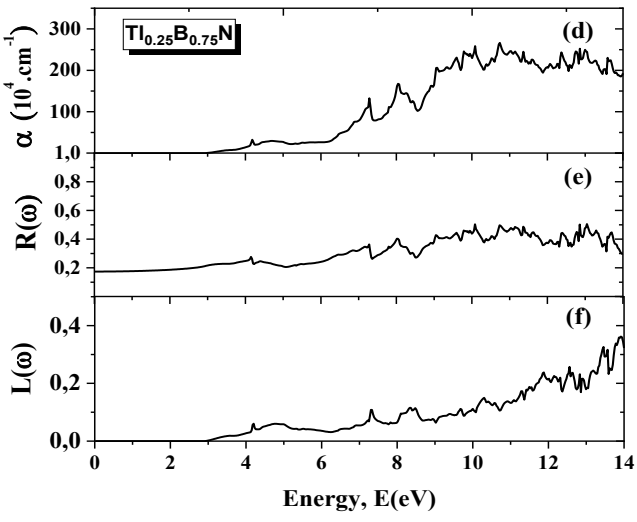


**Figure 9.** d, e, f. the absorption coefficient $\alpha(\omega)$, reflectivity R(ω), and energy loss function L(ω of the $Tl_{0.5}B_{0.5}N$ compound

## 4. Conclusion

In this work, a comprehensive first-principles investigation of the structural, electronic, and optical properties of $Tl_{1-x}B_xN$ alloys in the zinc-blende phase has been carried out for different boron concentrations (x = 0.25, 0.50, and 0.75). The structural optimization revealed a progressive decrease in the lattice parameter with increasing boron content, accompanied by a significant increase in the bulk modulus, indicating enhanced structural rigidity and stronger interatomic bonding. The calculated lattice parameters follow approximately Vegard's law, confirming the compositional dependence of the structural properties. The electronic band structure analysis shows a composition-dependent transition from semi-metallic to semiconducting behavior. Alloys with lower boron concentrations (x = 0.25 and 0.50) exhibit semi-metallic characteristics, whereas the composition with x = 0.75 displays a direct band gap of about 2.87 eV at the Γ point. The inclusion of spin–orbit coupling produces a slight reduction in the band gap but does not significantly modify the overall electronic character of the alloys. The calculated optical properties reveal a strong dependence on boron concentration. The evolution of the dielectric function, refractive index, absorption coefficient, reflectivity, and energy-loss spectra clearly reflects the underlying electronic structure. In particular, the absorption edge shifts toward higher photon energies as the boron content increases, consistent with the opening of the band gap.

The plasmon peaks observed in the energy-loss spectra further confirm the collective electronic excitations within the studied compounds.

Overall, the results demonstrate that tuning the boron concentration provides an effective strategy for controlling the electronic and optical response of $Tl_{1-x}B_xN$ alloys. The combination of tunable band gap, strong optical activity, and plasmonic features suggests that these materials could be promising candidates for advanced optoelectronic and photonic applications, including infrared detectors, optical sensors, and energy conversion devices. The present study provides valuable theoretical insights and reference data that may stimulate further theoretical and experimental investigations on thallium-based nitride alloys.

### Acknowledgments

I would like to express my sincere gratitude to all those who supported and assisted me throughout the completion of this work. Particularly Prof. Lachabi Abdelhadi and Dr. El Aid Abdelali, for their valuable contributions and insightful guidance, which greatly contributed to the success of this research.

**Authors Contribution**
All the authors have participated sufficiently in the intellectual content, conception and design of this work or the analysis and interpretation of the data, as well as the writing of the manuscript.

**Availability of data and materials**
Data will be made available upon reasonable request to the corresponding author.

**Conflict of interests**
The authors declare no conflict of interest.

## References


[1] Maryam.N, Sina. H.Study of ab ignition calculations of structural, electronic and optical properties of ternary semiconductor $Ga_{1-x}In_xSb$ alloys. Bulletin of Mterials Science, vol 47, 88;(2024). https://doi.org/10.1007/s1234-024-03177-5

[2] Leila. H, Akila. B, S. Touam. Show all 8 authors. Saad. B. First principles calculations of the structural, electronic, optical and thermal properties of $BN_xAs_{1-x}$ alloys. The philosophical Magazine A Journal of Theoretical Experimental and Applied Physics. 96(16): 1-18 (2016) https://doi.org/10.1080/14786435.2016.1177669

[3] A. M. Nikoo, H. Sadeghi, S. Javad Hashemifar, A. Arab. Ab initio calculation of structural, electronic, and optical properties of $Tl_xGa_{1-x}As$ ternaryalloys. Computational Condensed Matter. Vol 25, (2020), e00505. https://doi.org/10.1016/j.cocom.2020.e00505

[4] A. M. Nikoo, A. Arab & H. Sadeghi. Indian Journal of Physics, vol 96, 3527-3533, (2022)

[5] M. J. Winiarski. Electronic structure of wurtzite $Tl_xIn_{1-x}N$ alloys. Material Chemistry and physics, vol198,(2017),209-213. https://doi.org/10.1016/j.matchemphys.2017.06.005

[6] M. Belabbas, O. Arbouche, M. Zemouli, Y. Benallou, M. Benchehima, M.Ameri. Ab initio study of novel III-V nitride alloys $B_{1-x}Tl_xN$ for optoelectronic application. Computational condensed Matter, vol 16, (2018), e00309. https://doi.org/10.1016/j.cocom.2018.e00309

[7] S. Erden Gulebaglan. Fitst-principles investigation of structural and electronic properties of $Tl_xAl_{1-x}P$ ternary alloys. Journal of Taibah University for Science.(2021)15(1);486-492. https://doi.org/10.1080/16583655.2021.1991731

[8] Blaha,P, Schwarz ,k ;Madsen .G.K.H,kvasnicka ,D&Luitz , J (2001).WIEN2K:An augmented Plane Wave +Local Orbitals program for calculating Crystal Properties.Vienna university of technology .Available at: http://www.wien2k.at

[9] Perdew, J. P., Burke, K, & Ernzerhof, M (1996). Generalized Gradient Approximation Made simple .Physical Review Letters 77(18),3865-3868 https://doi.org/10.1103/physRevLett.77.3865

[10] Masek,J,Kudrnovsky , J.Maca ,F ,Drchal , V&Turek , l (2003) .Lattice constant in diluted magnetic semiconductors (Ga, Mn)As. physical Review B 67(15), 153203. https://doi.org/10.1103/physRevB.67153203

[11] Monkhorst, H.J&Pack,J.D(1976) special points for Brillouin-zone intergrations. Physical Review (1976). B, 13(12),5188-5192. https://doi.org/10.1103/physRevB.13.5188

[12] Lannoo ,M & Bourgion , J .(1981).Point Defects in Semiconductors l :Theoretical Aspects .Spring Seeries in solid-State sciences, Vol22,springer-Verlag ISBN:978-3-540-10868-5.

[13] Fox ,M.(2010).optical Properties of Solids ($2^{nd}$ ed).Oxford university Press.ISBN:978-0-19-957336-3

[14] M. Merabet, S. Benalia, L. Djoudi, O. Cheref, N. Bettahar, D. Rached, R. Belacel, Chinese Journal of Physics 60, 462 (2019). https://doi.org/10.1016/j.cjph.2019.05.026

[15] Claudia Ambrosch-Draxl, Jorge O. Sofo, Computer Physics Communications 175, 1 (2006). https://doi.org/10.1016/j.cpc.2006.03.005

[16] D. P. Rai, Sandeep, A. Shankar, Anup Pradhan Sakhya, T. P. Sinba, P. Grima-Gallardo, H. Cabrera, R. Khenata, Madhav Prasad Ghimire, J. R.K. Thapa, Journal of Alloys and Compounds 699, 1003-1011. (2017). https://doi.org/10.1016/j.jallcom.2016.12.443

[17] C. Kittel, Solid State Physics, Ed, Dunod university (1983) 287, 325.

[18] A.A.Adewak, A.Chik, T.Adam, T.M. Joshua, M.O.D urowoju, Optoelectronic behavior of ZnS Compound and its alloy: A first principle approach Mater. Today Commun. 27 (2021) 102077. https://doi.org/10.1016/j.mtcomm.2021.102077

[19] AlÙ, A, Silveirinha, M. G, Salndrino, A., & Engheta, N.(2007).Epsilon-near-zero metamaterials and electromagnetic sources: Tailoring the radiation phase pattem. Physical Review B, 75; 55410. https://doi.org/10.1103/PhysRevB.75.155410

[20] A.A.Adewale, A. A. Yahaya, L. O. Agbolade, O. K. Yusuffi, S. O. Azeez, K. K. Babalola, , K. O. Suleman, Y. K. Sanusi; A. Chik .Optoelectronic and mechanical

properties of gallium arsenide alloys: Based on density functional theory. Chemical Physics Impact 8 (2024) 100594.
https://doi.org/10.1016/j.ehphi.2024.100596

[21] Deobrat. S, Shivam. K, Sanjeev. K, Gupta & Yogesh. S. Single layer of carbon phosphyde as an efficient material for optoelectronic devices. Journal of Materials Science. Vol 53, 8314-8327, (2018).
https://doi.org/10.1007/s10853-018-2126-6

[22] Prangnell, L. (2016). Visible Light- Based Hurman Visual System Conceptual Model. arXiv preprint arXiv; 1609.04830.

[23] A. A. Sholagberu, W. A. Yahya, A. A Adwell, Pressure effects on the opto-electronic and mechanical properties of double perovskite $Cs_2$ $AgInCl_6$, Phys. Scr. 97 (2022) 085824
https://doi.org/10.1088/1402-4896/ac831d

[24] M. Marques, L. K. Teles, L. M. R. Scolfaro, and J. R. Leite, Appl. Phys. Lett. Vol. 83, Number 5 (2003)
https://doi.org/10.1063/1.1597986

[25] Liao, C.-H., AlQatari, F., & Li, X., « Band structures and direct-to-indirect bandgap transitions in BAlN and BGaN alloys: a first principle study » arXiv:2005.08274, 2020.
https://doi.org/10.48550/arXiv.2005.08274

[26] A. H. Reshak, Z. Charifi, H. Baaziz : The influence of the lattice relaxation on the optical properties of $GaN_xAs_{1-x}$ alloys, Solar Energy. V 90, P 134- 143. April2013.
https://doi.org/10.1016/j.solener.2012.12.015

[27] M. Tariq, MalakAzmat Ali, A. Laref, G. Murtaza .Anion replacement effect on the physical properties of metal halide double perovskites $Cs_2AgInX_6$ (X=F, Cl, Br, I). Volume State Communications, Volume 314- 315, Julz 2020, 113929.
https://doi.org/10.1016/j.cocom.2020.e00458

[28] Charifi Zoulikha, H. Baaziz Nadir Bouarissa. Predicted electronic properties of zonc- blende Zn1-xMgxSe alloys. April 2004. Material Chemistry and Physics 84(2-3) : 273-278.
https://doi.org/10.1016/S0254-0584(03)00377-8